Geophys. Astrophys. Fluid Dynamics, Vol. 85, pp. 163–194
Reprints available directly from the publisher
Photocopying permitted by license only

ON THE DISSIPATION OF INTERNAL SOLITONS IN COASTAL SEAS

PATRICK G. TIMKO and GORDON E. SWATERS[†]

Applied Mathematics Institute, Department of Mathematical Sciences, University of Alberta, Edmonton, Alberta, T6G 2G1 Canada

(Received 13 May 1996; In final form 21 October 1996)

Previous descriptions of the turbulent decay of an internal soliton have been based on an adiabatic assumption in which the soliton parameters continuously change in time in response to the dissipation. A complete leading order description of a decaying internal soliton including both horizontal and vertical dissipation is given. It is shown that the adiabatic ansatz fails to fully describe a decaying internal soliton under the influence of weak dissipation. Physically, the breakdown is the consequence of the fact that an adiabatically decaying internal soliton is unable to simultaneously satisfy averaged energy *and* mass balance relations. An extended region with vertical momentum flux develops behind the decaying soliton in order to compensate for the additional mass lost in the adiabatically decaying internal soliton. The leading order evolution of this extended region is described as is its connection to the stream function field associated with the internal soliton. The magnitude of the vertical flux associated with this region scales linearly with the dissipation parameters. The transition of this extended region back to zero is accomplished through the formation of a spatially decaying packet of linear internal gravity waves.

Keywords: Solitons; solitary waves; nonlinear waves; coastal oceanography; internal waves; internal tides

1. INTRODUCTION

Internal solitary waves in coastal seas can be produced by the interaction of tides and a shelf break (Briscoe, 1984). These large amplitude waves play an important role in the vertical transport of nutrients, and hence the biological cycle, in the shelf break region. For example, Sandstrom and Elliott (1984), in a study of the Nova Scotian

[†]Corresponding author. E-mail address gordon.swaters@ualberta.ca

shelf break region, argued that internal solitary waves were the dominant mixing mechanism by which nitrates were supplied to the upper mixed layer. It has been suggested (Briscoe, 1984) that up to 20% of the surface tidal energy can be dissipated as internal solitary waves. Specifically, Briscoe (1984), based on the Sandstrom and Elliott (1984) data, estimated that as much as approximately 50 mWm^{-2} is available for vertical mixing at the base of the mixed layer from tidally-generated internal solitary waves. Bogucki and Garrett (1993) have pointed out that this estimate is at least an order of magnitude larger than the energy input associated with internal wave dissipation or winds.

Unperturbed internal shelf-break solitons correspond to solutions of a *Korteweg de Vries* (KdV) equation which are compactly supported. That is, their amplitudes decay exponentially rapidly to zero both ahead and behind the steadily-travelling pulse of vertically deflected isopycnals. Thus, the mixing associated with an undisturbed internal soliton will be confined to the relatively narrow region containing the maximum isopycnal deflections. Presumably, physical oceanographic processes which can lead to the spatial and/or temporal enhancement of the vertical mixing associated with an internal soliton will have important biological consequences in as much as the horizontal extent of the upward nutrient fluxes will be increased (see, e.g., Fournier *et al.*, 1977).

One mechanism which can lead to enhanced vertical mixing is the dissipation of internal solitons (Farmer and Smith, 1978; Sandstrom *et al.*, 1989). The dissipation acts to extract energy out of the soliton pulses and increase the vertical mixing through widening the pycnocline (Bogucki and Garrett, 1993).

Several qualitative calculations have been presented to describe the dissipation of internal solitons (e.g., Koop and Browand, 1979; Lenone *et al.*,1982; Liu *et al.*,1982,1985; Liu, 1988; Bogucki and Garrett,1993). The key idea in these calculations is that the amplitude (and hence the speed) of the internal soliton decreases in accordance with an appropriate integrated energy balance relation. This approach, originally suggested by Ott and Sudan (1970), is based on a nonlinear WKB/geometrical optics or adiabatic ansatz in which, to quote Liu *et al.* (1985), "... the shape of the solitary wave ... does not change, but the wave parameters change slowly in time in accordance with the energy decay law".

This is true but it does not give a complete account of the dissipation of an internal soliton. The principal purpose of this paper is to present a complete leading order asymptotic description of a dissipating internal soliton. We shall show that while the above model calculations correctly describe the leading order adiabatic decay in the region of maximum isopycnal deflection, they neglect to describe an extended region of enhanced vertical momentum flux in the lee of the dissipating soliton. Although our work is motivated by observations of shelf break solitons, we will present a highly idealized calculation for a single soliton travelling over a flat bottom. In terms of direct applicability to shelf break solitons, our calculation can only be considered physically relevant long after the initial interaction of the tide with the shelf break in which the travelling solitons have separated from each other and the bottom depth appears slowly varying.

This region of enhanced vertical momentum flux in the lee of the dissipating soliton hereafter referred to, following Knickerbocker and Newell (1980b) or Kodama and Ablowitz (1980), as the shelf region[1], arises because an adiabatically dissipating internal soliton is unable to simultaneously satisfy the appropriate integrated energy and mass balance relations (Kaup and Newell, 1978) associated with the perturbed solitary wave equation. This shelf region corresponds to an extended region of vertically deflected isopycnals. We shall show that the vertical thickness associated with this shelf region scales linearly with the dissipation parameters and the horizontal length scales inversely with the dissipation parameters. Depending on the magnitude of the dissipation parameters, this region can allow for significant vertical momentum flux in the lee of the dissipating soliton. Eventually, of course, the amplitude of the soliton and thus the shelf region must decay to zero. We show that this is accomplished through the formation of a high wavenumber, within the context of the asymptotics associated with solitary waves, oscillatory wave tail which decays to zero.

We note here that Liu *et al.* (1985) and Liu (1988) retained only horizontal eddy viscosity terms in their analysis, arguing that these terms dominated the vertical eddy viscosity terms. Bogucki and

[1]The choice of the term shelf region is unfortunate from the view point of Oceanography since it confuses continental shelves with the property of perturbed solitary waves to generate an extended elevated region behind the propagating soliton. We have decided to use the terminology of soliton asymptotics to facilitate reference to that literature.

Garrett (1993) have questioned this point of view arguing that tidally-generated internal gravity waves tend to propagate in a region of relatively high vertical shear and that, as such, the vertical dissipation of energy cannot be neglected. In an attempt to address this problem, Bogucki and Garrett (1993) parameterized the dissipation parameter in terms of a flux Richardson number. Here, we describe the evolution of a dissipating internal soliton including both vertical and horizontal eddy viscosity and mass diffusivity terms in the governing equations. It is important to point out that our calculation does not address the decay of an internal soliton associated with the vertical shear induced by the soliton itself.

The plan of this paper is as follows. In Section 2 we briefly present the derivation of our model. In Section 3 we present a complete leading order asymptotic description of a weakly dissipating internal soliton. In Section 4 we discuss our results. The paper is summarized in Section 5.

2. PROBLEM FORMULATION

2.1. The Governing Equations

The underlying asymptotic assumptions leading to internal solitary waves are well known (see e.g., Benny, 1966) and thus our presentation will be very brief. The dimensional governing equations, under a Boussinesq approximation and with eddy viscosity terms, can be written in the form (see e.g., LeBlond and Mysak, 1978, see Fig. 1 for the geometry)

$$\rho^*_{t^*} + J^*(\psi^*, \rho^*) - \rho_* g^{-1} N^2(z^*)\psi^*_{x^*} = A_V \rho^*_{z^*z^*} + A_H \rho^*_{x^*x^*}, \tag{2.1}$$

$$\Delta^*\psi^*_{t^*} + J^*(\psi^*, \Delta^*\psi^*) = -\frac{g\rho^*_{x^*}}{\rho_*} + A_V \Delta^*\psi^*_{z^*z^*} + A_H \Delta^*\psi^*_{x^*x^*}, \tag{2.2}$$

where ψ^*, ρ^*, N and ρ_* are the dynamic stream function and density, Brunt-Väisälä frequency and the constant Boussinesq density fields, respectively. The right-handed coordinates (x^*, z^*) correspond to the horizontal and vertical coordinates, respectively, t^* is time, $\Delta^* = \partial_{x^*x^*} + \partial_{z^*z^*}, J^*(A,B) = A_{x^*}B_{z^*} - A_{z^*}B_{x^*}$, and g, A_H and A_V are the

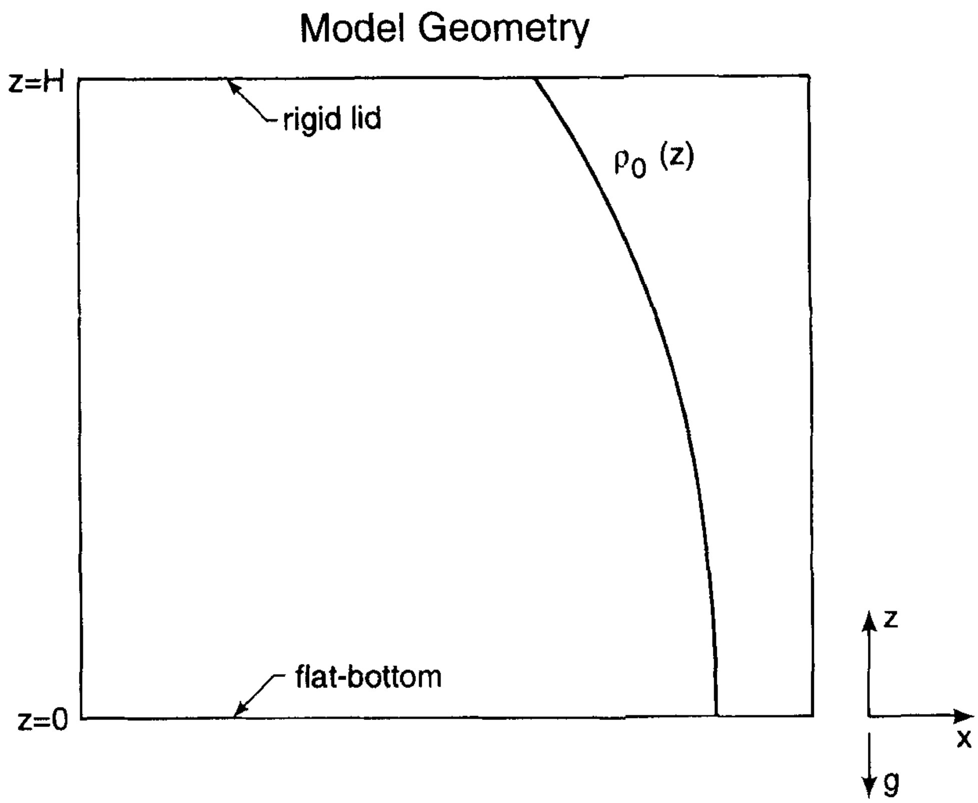

FIGURE 1 Geometry of the model considered here.

gravitational acceleration and the horizontal and vertical viscosities, respectively. The horizontal and vertical velocities, given by $\mathbf{u}^* = (u^*, w^*)$, respectively, are related to the stream function via $\mathbf{u}^* = \mathbf{e}_3 \times \nabla^* \psi^*$.

We have chosen to set the vertical and horizontal eddy viscosities in the mass conservation and vorticity equations equal to each other in order to reduce the number of coefficients in the subsequent analysis. This choice does not materially alter our conclusions. A similar crude approximation was introduced by LeBlond (1996) to study the dissipation of linear internal gravity waves.

Introduction into (2.1) and (2.2) of the nondimensional quantities

$$\left.\begin{aligned} x^* &= Lx, & t^* &= L(N^*H)^{-1}t, \\ z^* &= Hz, & \rho^* &= \varepsilon\rho_* H(N^*)^2 g^{-1}\rho, \\ S(z) &= (N/N^*)^2, & \psi^* &= \varepsilon N^* H^2 \psi, \\ \mu &= A_V L(\varepsilon H^3 N^*)^{-1}, & \nu &= A_H(\varepsilon L N^* H)^{-1}, \end{aligned}\right\} \qquad (2.3)$$

where $0 < \varepsilon = (H/L)^2 \ll 1$ with H and L the vertical and horizontal length scales, respectively, and where N^* is a characteristic Brunt-Väisälä frequency, together with the fast phase variable $\xi = x - ct$ and the slow time variable $T = -t$, leads to

$$c\rho_\xi + S(z)\psi_\xi = \varepsilon\{J(\psi, \rho) + \rho_T - \mu\rho_{zz} - \nu\rho_{xx}\}, \tag{2.4}$$

$$\rho_\xi - c\Delta\psi_\xi = \varepsilon\{\mu\Delta\psi_{zz} + \nu\Delta\psi_{xx} - J(\psi, \Delta\psi) - \Delta\psi_T\}, \tag{2.5}$$

where $\Delta = \partial_{zz} + \varepsilon\partial_{\xi\xi}$ and $J(A, B) = A_\xi B_z - A_z B_\xi$.

The assumption that $0 < \varepsilon \ll 1$, which corresponds to a long wavelength weakly nonlinear ansatz, is an appropriate approximation for shelf-break solitons. For example, echo sounder and CTD data presented by Sandstrom and Elliott (1984) and Sandstrom *et al.* (1989) for the Nova Scotian shelf suggest an internal soliton time scale of a few minutes and a typical Brunt-Väisälä frequency of about $2.5\times 10^{-2}\mathrm{s}^{-1}$. On the basis of the time scaling in (2.3), these suggest a horizontal length scale on the order of 1 km. The average depth of the water column in the Nova Scotia study area was about 160 m, implying that $\varepsilon \simeq 0.03$ which supports the long wavelength ansatz.

As for the scaling suggested in (2.3) for the amplitude of the dynamic density variations (and hence the stream function/dynamic pressure variations) associated with a shelf-break soliton, this is also consistent with the Nova Scotian shelf data. For example, potential density sections presented by Sandstrom and Elliott (1984) and Sandstrom *et al.* (1989) suggest a typical dynamic density variation of approximately $\rho^* \simeq 0.75\,\mathrm{kg/m^3}$ associated with the passage of a soliton implying that $\rho^*/\rho^* \simeq 7.3\times 10^{-4}$ where $\rho^* = 1025\,\mathrm{kg/m^3}$. The scaling for ρ^*/ρ^* in (2.3) is $\varepsilon H(N^*)^2 g^{-1} \simeq 3.2\times 10^{-4}$ which compares favorably to the estimate based directly on the observations.

We shall assume, for the moment, that the nondimensional horizontal and vertical eddy viscosities ν and μ, respectively, as defined in (2.3) are O(1) in magnitude. This assumption is more or less in agreement with the available observations. For example, if we use the Liu *et al.* (1985) estimate for A_H of $10\ \mathrm{m^2 s^{-1}}$, it follows that $\nu \simeq 0.1$.

The situation for the vertical eddy viscosity is a little more problematic. Sandstrom and Elliott (1984) and Sandstrom *et al.*

(1989) estimated that $A_V \simeq 10^{-4}–10^{-3}\mathrm{m}^2\mathrm{s}^{-1}$. This estimate suggests that $\mu \simeq 10^{-2}$. This estimate suggests that horizontal dissipation is more important than vertical dissipation in the dynamics of internal solitons. However, Bogucki and Garrett (1993) have argued that uncertainties in the physics and value of A_V make this conclusion somewhat doubtful. In particular, Bogucki and Garrett (1993) have argued that the appropriate vertical length scale to use in estimating μ is not the total depth of the water column but rather the thickness of the pycnocline region which contains the bulk of the soliton. In fact, if we follow this suggestion and calculate μ using $A_V \simeq 10^{-3}\mathrm{m}^2\mathrm{s}^{-1}$ and a value $H \simeq 15\,\mathrm{m}$, we find that $\mu \simeq 0.3$.

2.2. Derivation of the Perturbed KdV Equation

Inserting the expression

$$(\rho, \psi) = (\rho^{(0)}, \psi^{(0)}) + \varepsilon(\rho^{(1)}, \psi^{(1)}) + \mathrm{O}(\varepsilon^2), \tag{2.6}$$

into (2.4) and (2.5) leads to the O(1) and O(ε) problems, respectively,

$$\left.\begin{aligned} c\rho_\xi^{(0)} + S(z)\psi_\xi^{(0)} &= 0, \\ \rho_\xi^{(0)} - c\psi_{zz\xi}^{(0)} &= 0, \end{aligned}\right\}, \tag{2.7}$$

$$\left.\begin{aligned} c\rho_\xi^{(1)} + S(z)\psi_\xi^{(1)} &= J(\psi^{(0)}, \rho^{(0)}) + \rho_T^{(0)} - \mu\rho_{zz}^{(0)} - \nu\rho_{xx}^{(0)}, \\ \rho_\xi^{(1)} - c\psi_{zz\xi}^{(1)} &= \mu\psi_{zzzz}^{(0)} + \nu\psi_{zzxx}^{(0)} + c\psi_{\xi\xi\xi}^{(0)} - J(\psi^{(0)}, \psi_{zz}^{(0)}) - \psi_{zzT}, \end{aligned}\right\} \tag{2.8}$$

The O(1) equations may be combined to yield

$$\psi_{zz}^{(0)} + \frac{S(z)}{c^2}\psi^{(0)} = 0, \tag{2.9}$$

where we have integrated with respect to ξ exploiting the boundary condition $\psi^{(0)} \to 0$ as $x \to \pm\infty$. Assuming a separated solution for $\psi^{(0)}$ of the form

$$\psi^{(0)} = A(\xi, T)\phi(z), \tag{2.10}$$

leads to

$$\phi_{zz} + \frac{S(z)}{c^2}\phi = 0, \tag{2.11}$$

which, together with the rigid boundary conditions,

$$\phi(1) = \phi(0) = 0, \tag{2.12}$$

forms a Strum-Liouville eigenvalue problem for c.

The $O(\varepsilon)$ equations may be combined to yield

$$\begin{aligned}\psi^{(1)}_{zz\xi} + \frac{S(z)}{c^2}\psi^{(1)}_{\xi} = &\left[\frac{2\nu S}{c^3}A_{\xi\xi} - A_{\xi\xi\xi} - \frac{2S}{c^3}A_T\right]\phi \\ &-\frac{2S_z}{c^3}AA_{\xi}\phi^2 + \frac{2\mu}{c^3}A(S\phi)_{zz},\end{aligned} \tag{2.13}$$

where we have used the $O(1)$ solutions to simplify the inhomogeneous terms. Observing that $\psi^{(0)}$ is a proper solution to the homogeneous adjoint problem associated with (2.13) implies, as a consequence of the Fredholm Alternative Theorem (see e.g., Boyce and DiPrima, 1969), that

$$\int_0^1 \left\{\left[\frac{2\nu}{c^3}A_{\xi\xi} - A_{\xi\xi\xi} - \frac{2S}{c^3}A_T\right]\phi^2 - \frac{2S_z}{c^3}AA_{\xi}\phi^3 + \frac{2\mu}{c^3}A\phi(S\phi)_{zz}\right\}dz = 0,$$

must hold, which can be re-written in the form

$$A_T + \alpha AA_{\xi} + \beta A_{\xi\xi\xi} = -\gamma A + \nu A_{\xi\xi}, \tag{2.14}$$

where

$$\alpha = \frac{\int_0^1 S_z\phi^2 dz}{\int_0^1 S\phi^2 dz}, \tag{2.15}$$

$$\beta = \frac{c^3\int_0^1 \phi^2 dz}{2\int_0^1 S\phi^2 dz}, \tag{2.16}$$

$$\gamma = \frac{\mu \int_0^1 S^2(\phi_z)^2 dz}{c^2 \int_0^1 S\phi^2 dz} \geq 0. \tag{21.7}$$

Equation (2.14) is, of course, a perturbed KdV equation. We note that the Rayleigh-like and the Burgers-like damping terms $-\gamma A$ and $\nu A_{\xi\xi}$, respectively, in (2.14) arise exclusively to the vertical and horizontal eddy viscosity terms, respectively, in the governing equations.

If the fluid has constant stratification, i.e., S is constant, then it follows from (2.15) that $\alpha = 0$. In this case the evolution is not governed by the KdV equation (2.14), but rather by a higher order modified Korteweg-de Vries (mKdV) equation in which the quadratic nonlinear term in (2.14) is replaced with a cubic or higher order nonlinearity (see e.g., Gear and Grimshaw, 1983).

We choose an exponential model for the stratification function $S(z)$ so that $\alpha \neq 0$. Our specific choice for $S(z)$ is motivated by the stratification characteristics which exist on the Nova Scotian shelf during periods in which internal solitons have been observed (e.g. Sandstrom and Elliott, 1984; Sandstrom *et al.*,1989). The stratification can be reasonably well modelled (excluding the uppermost surface mixed layer) with an exponential function of the form

$$S(z) = S_0^2 \exp[\kappa(z-1)],$$

where S_0 and κ are the nondimensional Brunt-Väisälä frequency at $z = 1$ and inverse scale height, respectively.

The Sandstrom and Elliot (1984) study area had a depth of approximately 160 meters and was stably stratified with the Brunt-Väisälä frequency ranging from about $2.5 \times 10^{-2} s^{-1}$ near the surface till near zero at a depth of about 40 meters. Based on these observations we choose the vertical length scale to be $H = 160$ meters and reference Brunt-Väisälä frequency of $2.5 \times 10^{-2} s^{-1}$, suggesting values for S_0 and κ of approximately 1.0 and 4.0, respectively.

With the above exponential stratification function, the normalized vertical modes [i.e. the solutions to (2.11) and (2.12)] can be written in the form (Bryan and Ripa, 1978; Swaters and Mysak, 1985)

$$\phi_n(z) = E_n \left\{ Y_0\left(\frac{2S_0}{\kappa|c_n|}\right) J_0\left(\frac{2\sqrt{S(z)}}{\kappa|c_n|}\right) - J_0\left(\frac{2S_0}{\kappa|c_n|}\right) Y_0\left(\frac{2\sqrt{S(z)}}{\kappa|c_n|}\right) \right\},$$

with the eigenvalue relation

$$\mathrm{J}_0\left(\frac{2S_0\exp(-\kappa/2)}{\kappa|c_n|}\right)\mathrm{Y}_0\left(\frac{2S_0}{\kappa|c_n|}\right) - \mathrm{J}_0\left(\frac{2S_0}{\kappa|c_n|}\right)\mathrm{Y}_0\left(\frac{2S_0\exp(-\kappa/2)}{\kappa|c_n|}\right) = 0,$$

for $n=0,1,2,\ldots$, where the normalization constant E_n is chosen so that

$$\int_0^1 S(z)\phi_n(z)\phi_m(z)dz = \delta_{nm},$$

where J_0 and Y_0 are Bessel functions of the first and second kind of order zero, respectively.

In what follows we will focus on the rightward, i.e. $c>0$, solution. Our choice for the Brunt-Väisälä frequency will imply that $\alpha>0$ and $\beta>0$.

It is convenient to re-cast (2.14) into "standard" form. To this end we introduce the transformation

$$A(\xi, T) = -6(\beta^{1/3}/\alpha)\tilde{A}(\tilde{\xi}, T), \tag{2.18a}$$

$$\xi = \beta^{1/3}\tilde{\xi},\ \nu = \beta^{2/3}\tilde{\nu},\ \gamma = \delta\tilde{\nu}, \tag{2.18b}$$

into (2.14), yielding, after dropping the tildes,

$$A_T - 6AA_\xi + A_{\xi\xi\xi} = \nu(-\delta A + A_{\xi\xi}), \tag{2.19}$$

where we assume $\delta \simeq \mathrm{O}(1)$ and $0 \ll \varepsilon \ll \nu \ll 1$, i.e. the weak dissipation limit. Equation (2.19) is the form of the perturbed KdV equation we will henceforth work with.

3. STRUCTURE OF A DISSIPATING SOLITON

The spatial structure of a dissipating internal soliton is complex (see Fig. 2). In the co-moving region associated with the main pulse (i.e. region 1 in Fig. 2), the perturbed soliton can be described with a nonlinear WKB/geometrical optics asymptotic expansion, using the approach of Liu *et al.* (1985) or Bogucki and Garrett (1993). However,

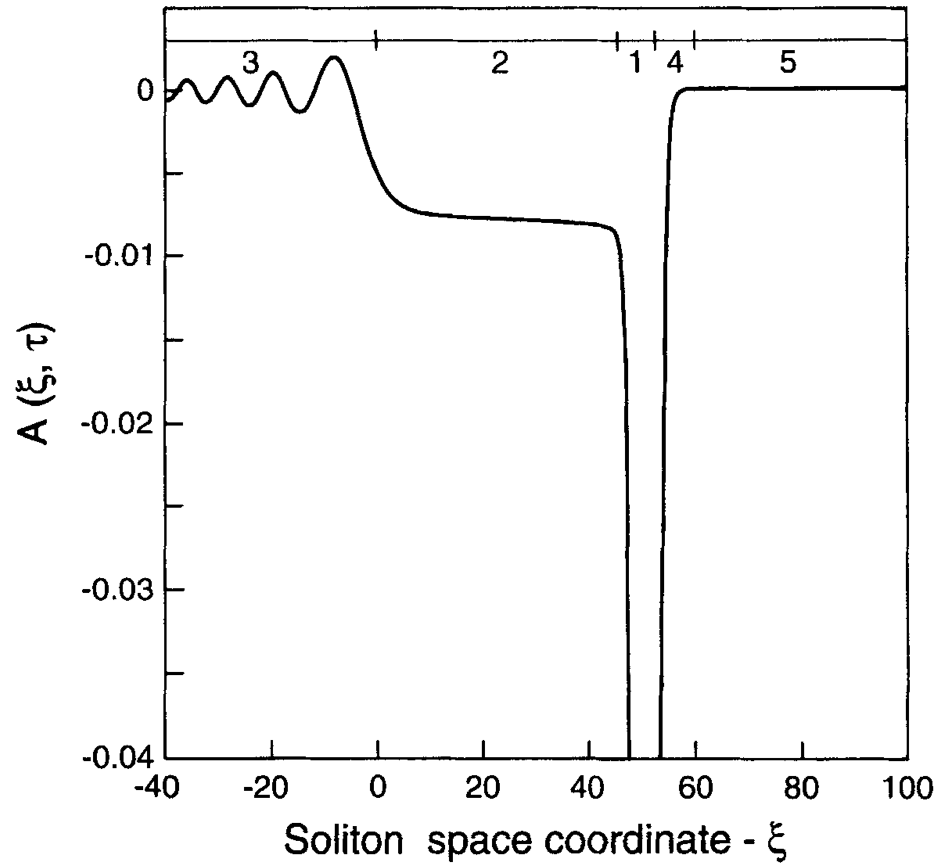

FIGURE 2 The spatial structure of a dissipating soliton. Region 1 is the main pulse region in which the soliton adjusts adiabatically. Region 2 is the shelf region. Region 3 is the wave tail region which describes the transition from the shelf to a zero background state. Regions 4 and 5 are ahead of the main pulse in which the adiabatic ansatz also breaks down.

as is known (e.g. Kodama and Ablowitz, 1980) and as we show below, a detailed calculation of the perturbation field in this main pulse region shows that this expansion is exponentially nonuniform behind the travelling soliton. Physically, this nonuniformity is the consequence of the formation of a "shelf" region behind the soliton (i.e. region 2 in Fig. 2) due to the fact that the adiabatically deforming soliton cannot simultaneously satisfy the appropriate mass and energy balances associated with the perturbed KdV equation (Kaup and Newell,1978; Knickerbocker and Newell,1980b).

The physical problem we examine here is an initial-value problem in which the soliton is initially unperturbed and centered about $x=0$. It follows that this shelf region can only extend a finite distance and must eventually approach zero. This transition is described by a small amplitude similarity solution to the perturbed KdV equation and has the appearance of a high wavenumber wave tail (see region 3 in Fig. 2) which smoothly merges with the shelf region and which decays to zero away from the main pulse.

3.1. Leading Order Evolution of the Main Pulse

In the absence of dissipation (i.e., $\nu=0$), the single soliton solution to (2.19) can be written in the form

$$A(\xi, T) = -2\eta^2 \operatorname{sech}^2 [\eta(\xi - 4\eta^2 T - \theta_0)], \tag{3.1}$$

where η and θ_0 are arbitrary amplitude and phase shift parameters, respectively.

Under a weak dissipation assumption, the evolution of the main pulse (given by region 1 in Fig. 2) can be described adiabatically (see e.g., Kaup and Newell, 1978; Grimshaw, 1979; Kodama and Ablowitz, 1980) in terms of a slowly-varying co-moving phase variable, denoted θ, and a slow time variable, denoted τ, given by respectively,

$$\left.\begin{aligned} \theta(\xi, T) &= \xi - 4\nu^{-1} \textstyle\int_0^{\nu T} \eta^2(s) ds, \\ \tau &= \nu T, \end{aligned}\right\} \tag{3.2}$$

and where we assume $\theta_0 = \theta_0(\tau)$ with $\theta_0(0) = 0$. Substitution of (3.2) into (2.19) leads to

$$-4\eta^2 A_\theta - 6AA_\theta + A_{\theta\theta\theta} = \nu[A_{\theta\theta} - \delta A - A_\tau]. \tag{3.3}$$

The solution to (3.3) is obtained in a straightforward asymptotic expansion of the form

$$A \simeq A^{(0)}(\theta, \tau) + \nu A^{(1)}(\theta, \tau) + \cdots. \tag{3.4}$$

Substitution of (3.4) into (3.3) leads, respectively, to the O(1) and O(ν) problems

$$-4\eta^2 A_\theta^{(0)} - 6A^{(0)} A_\theta^{(0)} + A_{\theta\theta\theta}^{(0)} = 0, \tag{3.5}$$

$$\mathscr{L}A^{(1)} = A^{(0)}_{\theta\theta} - \delta A^{(0)} - A^{(0)}_{\tau}, \tag{3.6}$$

where

$$\mathscr{L} \equiv \partial_{\theta\theta\theta} - (4\eta^2 + 6A^{(0)})\partial_\theta - 6A^{(0)}_\theta. \tag{3.7}$$

The solution to (3.5) is taken to be the soliton

$$A^{(0)}(\theta,\tau) = -2\eta^2(\tau)\,\mathrm{sech}^2\{\eta(\tau)[\theta - \theta_0(\tau)]\}. \tag{3.8}$$

Substituting this expression into (3.6) implies

$$\mathscr{L}A^{(1)} = A^{(0)}_{\theta\theta} - \delta A^{(0)} - \frac{\eta_\tau}{\eta}[2A^{(0)} + (\theta - \theta_0)A^{(0)}_\theta] - \theta_{0\tau}A^{(0)}_\theta. \tag{3.9}$$

The adjoint operator associated with $\mathscr{L}$, denoted $\mathscr{L}^A$, is given by

$$\mathscr{L}^A = 4\eta^2\partial_\theta + 6A^{(0)}\partial_\theta - \partial_{\theta\theta\theta}.$$

Observing that $A^{(0)}$ satisfies $\mathscr{L}^A A^{(0)} = 0$ implies that

$$\int_{-\infty}^{\infty}\left\{A^{(0)}_{\theta\theta} - \delta A^{(0)} - \frac{\eta_\tau}{\eta}[2A^{(0)} + (\theta - \theta_0)A^{(0)}_\theta] - \theta_{0\tau}A^{(0)}_\theta\right\}A^{(0)}\,d\theta = 0. \tag{3.10}$$

Alternatively, we may derive (3.10) within the context of a phase averaged or integrated energy balance approach. The energy balance equation associated with (3.3) may be written in the form

$$\left(-2\eta^2A^2 - 2A^3 + AA_{\theta\theta} - \frac{1}{2}A_\theta^2\right)_\theta = \nu A[A_{\theta\theta} - \delta A - A_\tau]. \tag{3.11}$$

If the expansion (3.4) is substituted into (3.11) and the result integrated with respect to θ over the interval $(-\infty,\infty)$, the leading order balance is

$$\int_{-\infty}^{\infty}[A^{(0)}_{\theta\theta} - \delta A^{(0)} - A^{(0)}_\tau]A^{(0)}\,d\theta = 0, \tag{3.12}$$

which is identical to (3.10) for $A^{(0)}$ given by (3.8).

If (3.8) is substituted into (3.10) and the integration carried out, one obtains

$$\eta_\tau = -\frac{2\delta\eta}{3} - \frac{8\eta^3}{15}, \tag{3.13}$$

the solution to which may be written in the form

$$\eta(\tau) = \left\{ \frac{5\delta\eta_0^2 \exp(-4\delta\tau/3)}{5\delta + 4\eta_0^2[1 - \exp(-4\delta\tau/3)]} \right\}^{1/2}, \tag{3.14}$$

where $\eta_0 = \eta(0) > 0$. From (3.14) we see that $\eta(\tau)$, and hence the amplitude of the soliton, decreases monotonically toward zero as τ increases (see Fig. 3a).

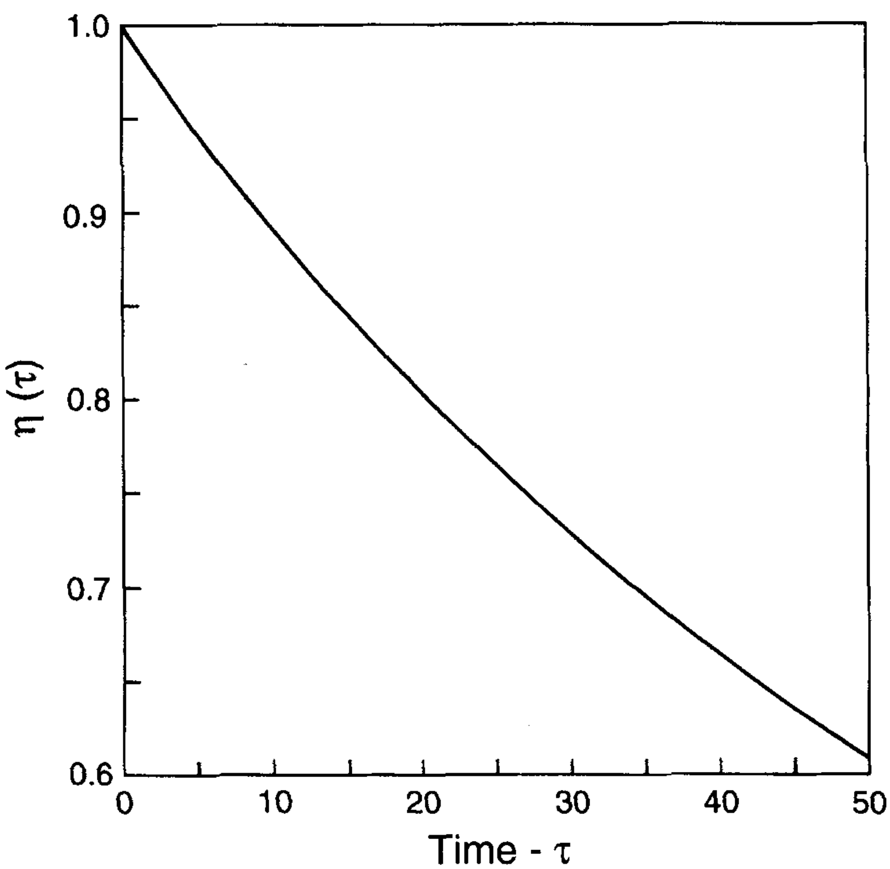

FIGURE 3 The amplitude parameter $\eta(\tau)$ and (b) the phase shift parameter $\theta_0(\tau)$ for $\eta_0 = \delta = 1$.

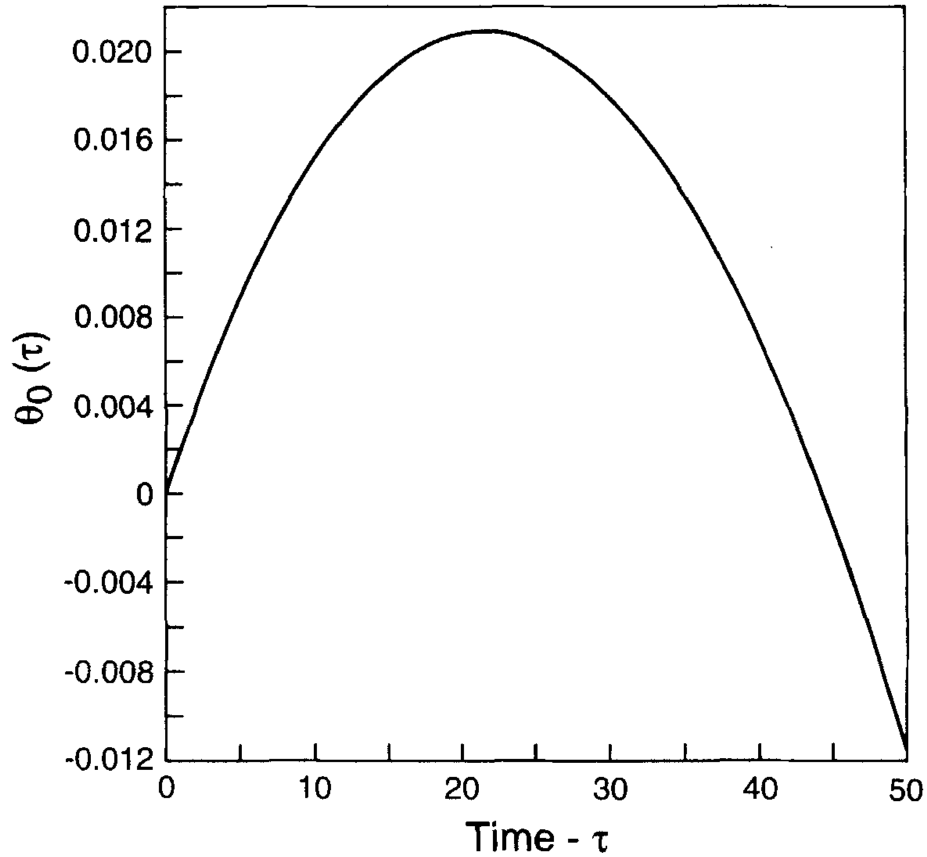

FIGURE 3 (Continued)

We can see how, according to this model, vertical and horizontal eddy dissipation leads to a qualitatively different temporal decay in the soliton amplitude. If horizontal eddy dissipation is neglected [i.e. neglecting the $A_{\theta\theta}$ term in (3.3)] and one retains only vertical eddy dissipation, it will follow that the soliton amplitude will decay exponentially rapidly. This is consistent with the result of Bogucki and Garrett (1993). On the other hand, if vertical eddy dissipation is neglected (i.e. $\delta = 0$) in (3.3) and only horizontal eddy dissipation is retained, it follows that the soliton amplitude, which is proportional to η^2, will decay algebraically. For equal values of the dissipation parameters γ and ν, the vertical eddy viscosity term will lead to a much more rapid decay in the solitary wave compared to the horizontal eddy viscosity term. This point is important because it lends support to Bogucki and Garrett's (1993) contention that vertical momentum diffusion cannot be neglected in the dissipation of an internal soliton.

The above first-order solvability conditions do not determine the evolution of the phase shift $\theta_0(\tau)$. This parameter is determined by higher order solvability conditions (Karpman and Maslov,1978). Here we do not carry out this additional calculation but simply point out that the inverse scattering formalism developed by Karpman and Maslov for a perturbed KdV equation implies that $\theta_0(\tau)$ satisfies

$$\frac{\partial\theta_0}{\partial\tau} = -(4\eta^3)^{-1}\int_{-\infty}^{\infty}[-\delta A^{(0)}(s,\tau) + A^{(0)}_{\theta\theta}(s,\tau)]\mathscr{K}(s)\,ds, \tag{3.15}$$

where the integration variable $s=\eta(\theta-\theta_0)$ with $A^{(0)}(s,\tau) = -2\eta^2(\tau)$ $\text{sech}^2(s)$ and

$$\mathscr{K}(s) = s\,\text{sech}^2(s) + \tanh(s) + \tanh^2(s).$$

Substitution of (3.8) into (3.15) leads to

$$\frac{\partial\theta_0}{\partial\tau} = \frac{8\eta^2(\tau) - 5\delta}{15\eta(\tau)}. \tag{3.16}$$

If (3.14) is used to eliminate $\eta(\tau)$ in (3.16), it follows assuming $\theta_0(0) = 0$, after a little algebra, that

$$\begin{aligned}\theta_0(\tau) = (5\delta)^{-1}\Bigg\{&3\arcsin\left[\left(\frac{4\eta_0^2}{5\delta+4\eta_0^2}\right)^{1/2}\right]\\ &-3\arcsin\left[\left(\frac{4\eta_0^2\exp(-4\delta\tau/3)}{5\delta+4\eta_0^2}\right)^{1/2}\right]\\ &+\left[\frac{5\delta}{4\eta_0^2}\right]^{1/2} - \left[\frac{5\delta+4\eta_0^2[1-\exp(-4\delta\tau/3)]}{4\eta_0^2\exp(-4\delta\tau/3)}\right]^{1/2}\Bigg\}.\end{aligned} \tag{3.17}$$

In Figure 3b we plot $\theta_0(\tau)$ vs. τ for $\eta_0 = \delta = 1$. Initially, $\theta_0(\tau)$ is positive after which it becomes increasingly negative.

3.2. The Perturbation Field in the Main Pulse

Equation (3.9) may be integrated with respect to θ to give

$$\begin{aligned}&\{-4\eta^2+12\eta^2\text{sech}^2[\eta(\theta-\theta_0)]+\partial_{\theta\theta}\}A^{(1)}=\\&\frac{(44\eta^3-10\delta\eta)}{15}\tanh[\eta(\theta-\theta_0)]-4\eta^3\tanh^3[\eta(\theta-\theta_0)]\\&+\frac{[(20\delta\eta^2-16\eta^4)(\theta-\theta_0)-30\theta_{0\tau}\eta^2]}{15}\text{sech}^2[\eta(\theta-\theta_0)]+\Gamma(\tau),\end{aligned}\tag{3.18}$$

where we have used (3.8) and (3.13) and where $\Gamma(\tau)$ is a constant of integration with respect to θ. To determine $\Gamma(\tau)$ we impose the boundary condition that ahead of the dissipating soliton the solution smoothly vanishes, i.e. $\lim_{\theta\to\infty}A^{(1)}(\theta,\tau)=0$. Taking this limit in (3.18) implies

$$\Gamma(\tau)=\frac{16\eta^3+10\delta\eta}{15}.\tag{3.19}$$

However substitution of (3.19) into (3.18) and taking the limit $\theta\to-\infty$, implies

$$\lim_{\theta\to-\infty}A^{(1)}(\theta,\tau)=-\frac{8\eta^2+5\delta}{15\eta}\neq 0,\tag{3.20}$$

that is, the perturbation field $A^{(1)}(\theta,\tau)$ does not approach zero behind the dissipating soliton but rather a relatively constant nonzero value corresponding to the formation of the "shelf" region. The limit (3.20) implies that the asymptotic expansion (3.4) is exponentially nonuniform behind the dissipating soliton.

Physically, the shelf region arises because the asymptotic expansion (3.4) is unable to simultaneously satisfy the globally integrated energy and mass balances for (3.3) (see e.g., Grimshaw, 1979; Knickerbocker and Newell, 1980b; Kodama and Newell, 1980).

The mass balance equation for (3.3) may be written in the form

$$[-4\eta^2A-3A^2+A_{\theta\theta}]_\theta=\nu[A_{\theta\theta}-\delta A-A_\tau].\tag{3.21}$$

If the expansion (3.4) is substituted into (3.21) and the result integrated with respect to θ over the interval $(-\infty,\infty)$, the leading order balance is

$$\int_{-\infty}^{\infty} [\delta A^{(0)} + A_\tau^{(0)}] d\theta = 0. \tag{3.22}$$

It is not possible to determine the evolution of the slowly dissipating soliton amplitude and phase parameters such that both (3.12) and (3.22) hold. Thus, given that $\eta(\tau)$ and $\theta_0(\tau)$ are determined from energy balance considerations, as is known theoretically based on the inverse scattering formalism for the perturbed KdV equation (Kaup and Newell, 1978), it follows that the adiabatically dissipating internal soliton cannot satisfy the appropriate mass balance relation. The shelf region forms to compensate for the extra mass lost in the adiabatically dissipating main pulse region.

We complete this subsection by determining $A^{(1)}(\theta,\tau)$ following the methods of Kodama and Ablowitz (1980) and Swaters and Sawatzky (1989). If (3.19) is substituted into (3.18) with the new independent variable

$$\zeta = \tanh[\eta(\theta - \theta_0)],$$

one obtains

$$\left[\left(1-\zeta^2\right)A_\zeta^{(1)}\right]_\zeta + \left[12 - \frac{4}{(1-\zeta^2)}\right]A^{(1)} = -2\theta_{0\tau}$$
$$+\frac{(60\zeta^2+60\zeta+16)\eta^2+10\delta}{15\eta(1+\zeta)} + \frac{10\delta-8\eta^2}{15\eta}\ln\left(\frac{1+\zeta}{1-\zeta}\right). \tag{3.23}$$

Observing that a homogeneous solution to (3.23) is the associated Legendre function $P_3^2(\zeta)=15\zeta(1-\zeta^2)$ allows one to construct a variation of parameter solution in the form $A^{(1)}=\Phi(\zeta,\tau)P_3^2(\zeta)$. Substitution of this form into (3.23) leads, after some algebra, to

$$\left[\zeta^2\left(1-\zeta^2\right)^3\Phi_\zeta\right]_\zeta = \frac{2\delta}{45\eta}\zeta(1-\zeta) + \frac{\eta}{225}(16\zeta+44\zeta^2-60\zeta^4)$$
$$+\frac{10\delta-8\eta^2(1+\zeta)}{225\eta}\zeta(1-\eta)\ln\left(\frac{1+\zeta}{1-\zeta}\right) - \frac{2\zeta(1-\zeta^2)\theta_{0\tau}}{15}. \tag{3.24}$$

If equation (3.24) is integrated twice with respect to ζ, with the integration constants chosen so that $A^{(1)}\to 0$ as $\zeta\to 1$ (i.e., $\theta\to +\infty$), it follows, after some algebra (for details see Timko, 1995), that

$$\begin{aligned}A^{(1)} = \frac{\delta}{6\eta}\Big[&2+\zeta-3\zeta^2-\frac{3}{2}\zeta(1-\zeta^2)\ln\left(\frac{1+\zeta}{1-\zeta}\right)\\&+(1-\zeta^2)\ln\left(\frac{1+\zeta}{1-\zeta}\right)-\frac{1}{4}\zeta(1-\zeta^2)\ln^2\left(\frac{1+\zeta}{1-\zeta}\right)\Big]\\&+\frac{\eta}{15}\Big[8+4\zeta-12\zeta^2-6\zeta(1-\zeta^2)\ln\left(\frac{1+\zeta}{1-\zeta}\right)\\&-2(1-\zeta^2)\ln\left(\frac{1+\zeta}{1-\zeta}\right)+\frac{1}{2}\zeta(1-\zeta^2)\ln^2\left(\frac{1+\zeta}{1-\zeta}\right)\Big]\\&+\frac{\theta_{0\tau}}{2}\Big[-1+\zeta^2+\frac{1}{2}\zeta(1-\zeta^2)\ln\left(\frac{1+\zeta}{1-\zeta}\right)\Big],\end{aligned}\tag{3.25}$$

which can be re-writtern in the form

$$\begin{aligned}A^{(1)}(\theta,\tau) = \frac{\delta}{6\eta}\{&3\operatorname{sech}^2\phi[1-\phi\tanh\phi]-1\\&+\tanh\phi-\phi\operatorname{sech}^2\phi[\phi\tanh\phi-2]\}\\&+\frac{\eta}{15}\{12\operatorname{sech}^2\phi[1-\phi\tanh\phi]-4\\&+4\tanh\phi+2\phi\operatorname{sech}^2\phi[\phi\tanh\phi-2]\}\\&+\frac{\theta_{0\tau}}{2}\{\operatorname{sech}^2\phi[1-\phi\tanh\phi]\},\end{aligned}\tag{3.26}$$

where, for convenience, we have introduced $\phi=\eta(\theta-\theta_0)$.

From (3.26) we see that as $(\theta-\theta_0)\to+\infty$,

$$A^{(1)}(\theta,\tau)\simeq\frac{\eta(8\eta^2-10\delta)}{15}(\theta-\theta_0)^2\exp\left[-2\eta(\theta-\theta_0)\right],\tag{3.27}$$

whereas, as $(\theta-\theta_0)\to-\infty$,

$$A^{(1)}(\theta,\tau)\simeq-\frac{8\eta^2+5\delta}{15\eta}-\frac{\eta(8\eta^2-10\delta)}{15}(\theta-\theta_0)^2\exp\left[2\eta(\theta-\theta_0)\right].\tag{3.28}$$

From (3.8) and (3.27), we see that

$$\left|\frac{A^{(1)}(\theta,\tau)}{A^{(0)}(\theta,\tau)}\right| \simeq \mathrm{O}[(\theta-\theta_0)^2],$$

for $(\theta - \theta_0) \rightarrow +\infty$. Thus the asymptotic expansion (3.4) is algebraically nonuniform ahead of the dissipating soliton. The algebraic nonuniformity ahead of the dissipating soliton can be removed by constructing a hybrid WKB/similarity solution for the soliton region ahead of the main pulse (see e.g., Kodama and Ablowitz, 1980 and Timko, 1995) which is not needed here.

The situation behind the main pulse is far more complex. From (3.8) and (3.28), we see that

$$\begin{aligned} A(\theta,\tau) &\simeq A^{(0)}(\theta,\tau) + \nu A^{(1)}(\theta,\tau) + \mathrm{O}\,(\nu^2) \\ &\rightarrow -\frac{\nu[8\eta^2(\tau)+5\delta]}{15\eta(\tau)} + \mathrm{O}(\nu^2), \end{aligned} \tag{3.29}$$

as $(\theta - \theta_0) \rightarrow -\infty$. As written, (3.29) contradicts the implicit assumption that the internal soliton is initially undistorted implying that the shelf region can only be of finite extent subsequently. Equation (3.29) suggests that the mass, which is proportional to $\int_{-\infty}^{\infty} A(\theta,\tau)d\theta$, is infinite which is, of course, physical nonsense since the mass is initially finite.

3.3. The Shelf Region

The evolution of the shelf region is described a solution to (2.19) of the form

$$A = \nu\tilde{A}(\chi,\tau), \tag{3.30}$$

where we have introduced the stretched phase variable $\chi = \nu\xi$ and τ is given as before. Substitution of (3.30) into (2.19) leads to

$$\tilde{A}_\tau + \delta\tilde{A} = 6\nu\tilde{A}\tilde{A}_\chi + \nu^2(\tilde{A}_{\chi\chi} - \tilde{A}_{\chi\chi\chi}). \tag{3.31}$$

Assuming a straightforward asymptotic expansion for $\tilde{A}(\chi, \tau)$ of the form

$$\tilde{A}(\chi, \tau) \simeq \tilde{A}^{(0)}(\chi, \tau) + O(\nu), \tag{3.32}$$

leads to the leading order problem

$$\tilde{A}^{(0)}_{\tau} = -\delta \tilde{A}^{(0)}, \tag{3.33}$$

which has the general solution

$$\tilde{A}^{(0)}(\chi, \tau) = \Upsilon(\chi) \exp(-\delta\tau). \tag{3.34}$$

The function $\Upsilon(\chi)$ must be chosen so that $\tilde{A}^{(0)}(\chi, \tau)$ asymptotically matches the leading order structure of the propagating main pulse in the far field behind the main pulse. Since we have assumed that there is no phase shift initially (so that soliton is centered on $\xi = 0$), it follows from (3.2) that, to leading order and in terms of χ, the position of the main pulse at time τ, denoted as $\chi_c(\tau)$, will be given by

$$\begin{aligned} \chi_c(\tau) &= 4 \int_0^{\tau} \eta^2(s)\, ds \\ &= \frac{15}{4} \ln\left\{1 + \frac{4\eta_0^2}{5\delta}[1 - \exp(-4\delta\tau/3)]\right\}, \end{aligned} \tag{3.35}$$

where we have used (3.14). The appropriate boundary condition for $\tilde{A}^{(0)}(\chi, \tau)$ is therefore

$$\tilde{A}^{(0)}(\chi_c(\tau), \tau) = -\frac{8\eta^2(\tau) + 5\delta}{15\eta(\tau)}, \tag{3.36}$$

which corresponds to the leading order amplitude of the main pulse in the far field behind the main pulse.

Substitution of (3.34) into (3.36) implies that $\Upsilon(\chi)$ is given by

$$\Upsilon(\chi) = -\frac{\{8\eta^2[\tau_c(\chi)] + 5\delta\} \exp[\delta\tau_c(\chi)]}{15\eta[\tau_c(\chi)]}, \tag{3.37}$$

where $\tau_c(\chi)$ is the inverse function associated with $\chi_c(\tau)$, given by

$$\tau_c(\chi) = -\frac{3}{4\delta}\ln\left\{1 + \frac{5\delta}{4\eta_0^2}[1 - \exp(4\chi/15)]\right\}. \tag{3.38}$$

Thus, in summary, the leading order evolution of the dissipating soliton in the shelf region interval $0 < \xi \leq \nu^{-1}\chi_c(\nu T)$ is given by

$$A(\xi, T) \simeq -\frac{\nu\{8\eta^2[\tau_c(\nu\xi)] + 5\delta\}}{15\eta[\tau_c(\nu\xi)]} \exp\{\delta[\tau_c(\nu\xi) - \nu T]\} + O(\nu^2), \tag{3.39}$$

and zero elsewhere and where, to facilitate constructing an uniformly valid leading order solution, we have chosen to write the solution with respect to ξ and T.

3.4. The Dispersive Wave Tail

The transition from the shelf back to zero occurs in a relatively small region centered about $\xi = 0$ and is described by a solution to (2.19) of the form

$$A = \nu\hat{A}(\xi, T; \tau). \tag{3.40}$$

Substitution of (3.30) into (2.19) leads to

$$\hat{A}_T + \hat{A}_{\xi\xi\xi} = \nu(6\hat{A}\hat{A}_\xi - \hat{A}_\gamma - \delta\hat{A} + \hat{A}_{\xi\xi}). \tag{3.41}$$

Assuming a straightforward asymptotic expansion for $\hat{A}(\xi, T; \tau)$ of the form

$$\hat{A}(\xi, T; \tau) \simeq \hat{A}^{(0)}(\xi, T; \tau) + O(\nu), \tag{3.42}$$

leads to the leading order problem

$$\hat{A}_T^{(0)} + \hat{A}_{\xi\xi\xi}^{(0)} = 0. \tag{3.43}$$

The appropriate boundary and asymptotic matching conditions associated with (3.43) are

$$\lim_{\xi \to -\infty} \hat{A}^{(0)}(\xi, T; \tau) = 0, \tag{3.44}$$

$$\lim_{\xi \to +\infty} \hat{A}^{(0)}(\xi, T; \tau) = \lim_{\chi \to 0^+} \tilde{A}^{(0)}(\chi, \tau), \tag{3.45}$$

where $\tilde{A}^{(0)}(\chi, \tau)$ is given by (3.34), (3.37) and (3.38).

The solution to (3.43) which can satisfy (3.44) and (3.45) is a similarity solution in the form (Knickerbocker and Newell, 1980b)

$$\left.\begin{aligned} \hat{A}^{(0)} &= \Psi(\lambda, \tau), \\ \lambda &= \xi(3T)^{-1/3}. \end{aligned}\right\} \tag{3.46}$$

Substitution of (3.46) into (3.43) leads to

$$\Psi_{\lambda\lambda\lambda} - \lambda \Psi_\lambda = 0, \tag{3.47}$$

which has the general bounded solution

$$\Psi(\lambda, \tau) = \varphi_0(\tau) + \varphi_1(\tau) \int_{-\infty}^{\lambda} \mathrm{Ai}(s)\, ds, \tag{3.48}$$

where $\mathrm{Ai}(s)$ is the bounded Airy function and where $\varphi_0(\tau)$ and $\varphi_1(\tau)$ are constants of integration with respect to λ. Application of (3.44) and (3.45) implies $\varphi_0(\tau) = 0$ and

$$\varphi_1(\tau) = -\frac{8\eta_0^2 + 5\delta}{15\eta_0} \exp(-\delta\tau), \tag{3.49}$$

respectively, since $\int_{-\infty}^{\infty} \mathrm{Ai}(s)\, ds = 1$.

Thus, in summary, the leading order evolution of the dissipating soliton in the transition or wave tail region $-\infty < \xi \simeq 0$ is given by

$$A(\xi, T) \simeq -\frac{\nu(8\eta_0^2 + 5\delta)}{15\eta_0} \exp(-\nu\delta T) \left[\int_{-\infty}^{\xi(3T)^{-1/3}} \mathrm{Ai}(s)\, ds \right], \tag{3.50}$$

for $T>0$ where, to facilitate constructing an uniformly valid leading order solution, we have chosen to write the solution with respect to ξ and T.

4. DISCUSSION

To begin, we need an uniformly valid representation of the solution, which we denote as $A_{\text{unif}}(\xi,T)$. This is achieved by adding together all of the individual asymptotic contributions associated with the main pulse, shelf region and dispersive wave tail and subtracting the leading order overlap between each subregion. That is,

$$A_{\text{unif}}(\xi,T) = \overbrace{(3.8)+\nu(3.26)}^{\text{main pulse region}} + \overbrace{(3.39)}^{\text{shelf region}} + \overbrace{(3.50)}^{\text{wave tail region}}$$
$$+ \overbrace{\frac{\nu[8\eta^2(\nu T)+5\delta]}{15\eta(\nu T)}}^{\text{main pulse and shelf overlap}} + \overbrace{\frac{\nu(8\eta_0^2+5\delta)\exp(-\delta\nu T)}{15\eta_0}}^{\text{shelf and wave tail overlap}}, \tag{4.1}$$

or, written out fully,

$$\begin{aligned} A_{\text{unif}}(\xi,T) &= -2\eta^2(\nu T)\operatorname{sech}^2\phi \\ &+\nu\Bigg[\frac{\delta}{6\eta(\nu T)}\{3\operatorname{sech}^2\phi[1-\phi\tanh\phi]-1 \\ &\qquad +\tanh\phi-\phi\operatorname{sech}^2\phi[\phi\tanh\phi-2]\} \\ &+\frac{\eta(\nu T)}{15}\{12\operatorname{sech}^2\phi\,[1-\phi\tanh\phi]-4 \\ &\qquad +4\tanh\phi+2\phi\operatorname{sech}^2\phi[\phi\tanh\phi-2]\} \\ &+\frac{[8\eta^2(\nu T)-5\delta]}{30\eta(\nu T)}\{\operatorname{sech}^2\phi[1-\phi\tanh\phi]\} \\ &-\frac{\{8\eta^2[\tau_c(\nu\xi)]+5\delta\}}{15\eta[\tau_c(\nu\xi)]}\exp\{\delta[\tau_c(\nu\xi)-\nu T]\} \\ &-\frac{(8\eta_0^2+5\delta)}{15\eta_0}\exp(-\nu\delta T)\left[\int_{-\infty}^{\xi(3T)^{-1/3}}\operatorname{Ai}(s)\,ds\right] \\ &+\frac{[8\eta^2(\nu T)+5\delta]}{15\eta(\nu T)}+\frac{\nu(8\eta_0^2+5\delta)\exp(-\delta\nu T)}{15\eta_0}\Bigg], \end{aligned} \tag{4.2}$$

where $\phi = \eta(\nu T)[\theta(\xi, T) - \theta_0(\nu T)$ with $\theta(\xi, T), \eta(\nu T), \theta_0(\nu T)$ and $\tau_c(\nu\xi)$ given by (3.2), (3.14), (3.17) and (3.38), respectively.

In Figure 4, we depict $A_{\text{unif}}(\xi,T)$ for a sequence of T values assuming $\nu = 0.01$ and $\delta = \eta_0 = 1.0$. We have chosen this value of ν in order to be able to effectively illustrate the theory while maintaining some semblance of asymptotic consistency. The initial undistorted soliton is shown in Figure 4a and we show $A_{\text{unif}}(\xi,T)$ for $T = 3000$, i.e., $\tau = 30$, in Figure 4b. In order to accentuate the shelf and wave tail region we show only that portion of $A_{\text{unif}}(\xi,T)$ greater than -0.04. As the dissipating soliton moves from left to right one can see the development of the shelf region extending from the main pulse to about $\xi = 0$ and the oscillatory wave tail which appears to begin at about $\xi = 0$ extending into the $\xi < 0$ region. As time increases the relative wavelength of the oscillations increases.

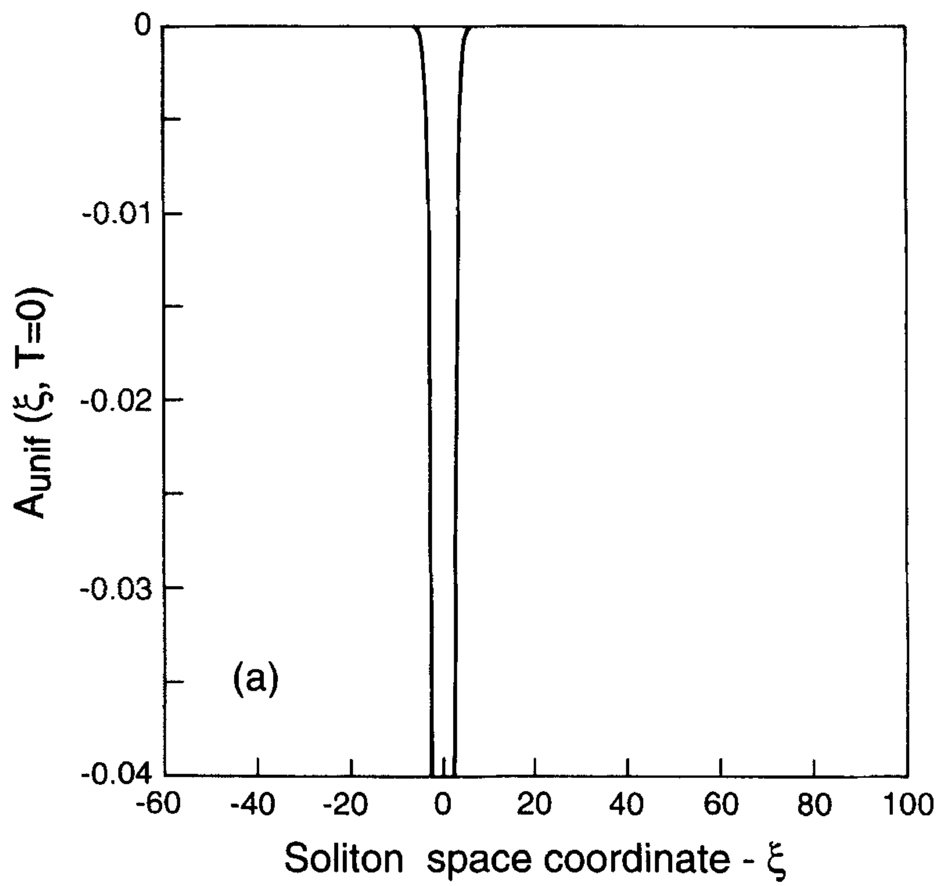

FIGURE 4 The uniformly valid solution $A_{\text{unif}}(\xi,T)$ for (a) $T = 0$ and (b) $T = 3000$ with $\nu = 0.01$, respectively. In order to emphasize the wave tail region we only show values greater than -0.04.

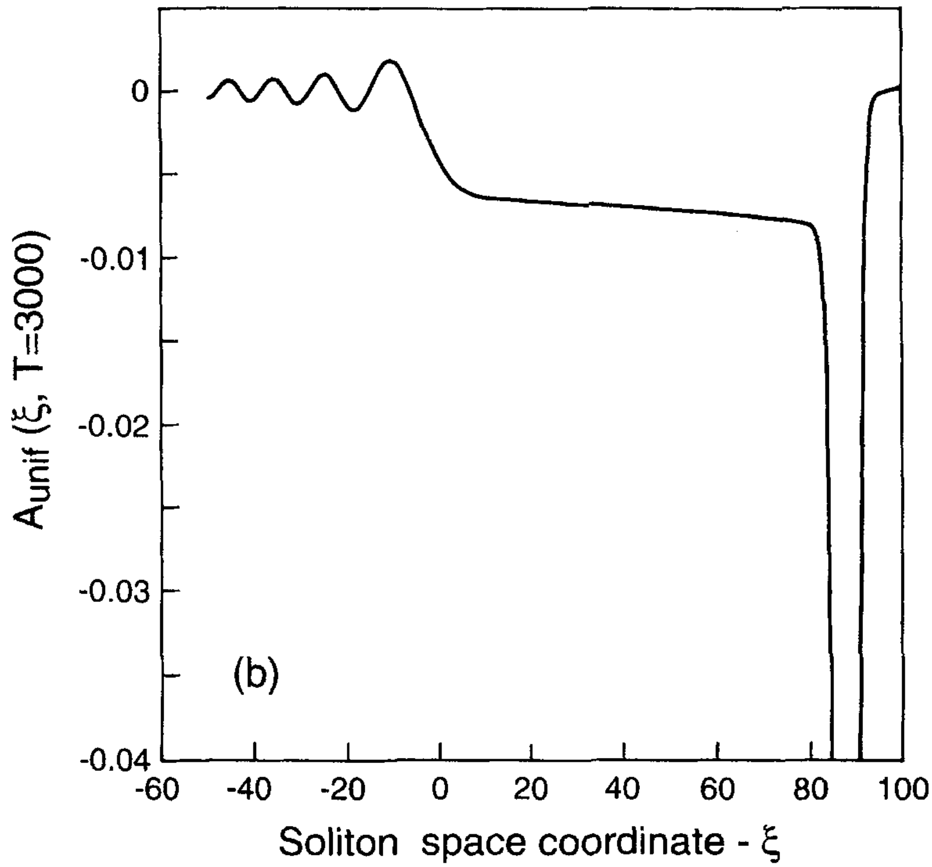

FIGURE 4 (Continued)

In Figure 5 we show gray-scale plots of the uniformly valid stream function, denoted $\psi_{\text{unif}}(z, \xi, T)$, given by

$$\psi_{\text{unif}}(z, \xi, T) = A_{\text{unif}}(\xi, T)\phi_0(z), \tag{4.3}$$

where $\phi_0(z)$ is the gravest vertical normal mode for the same sequence of times and parameter values as in Figure 4. Because there is a marked difference in the amplitude of the main pulse region and the shelf/tail region we found gray-scale rather than contour plots a better illustrator of the stream function field. The gray-scale intensity scales linearly with the magnitude of the stream function. The shelf region is the horizontally elongated shaded region in Figure 5b directly behind the main pulse which appears relatively dark. The wave tail region corresponds to the small number of vertically elongated lightly shaded

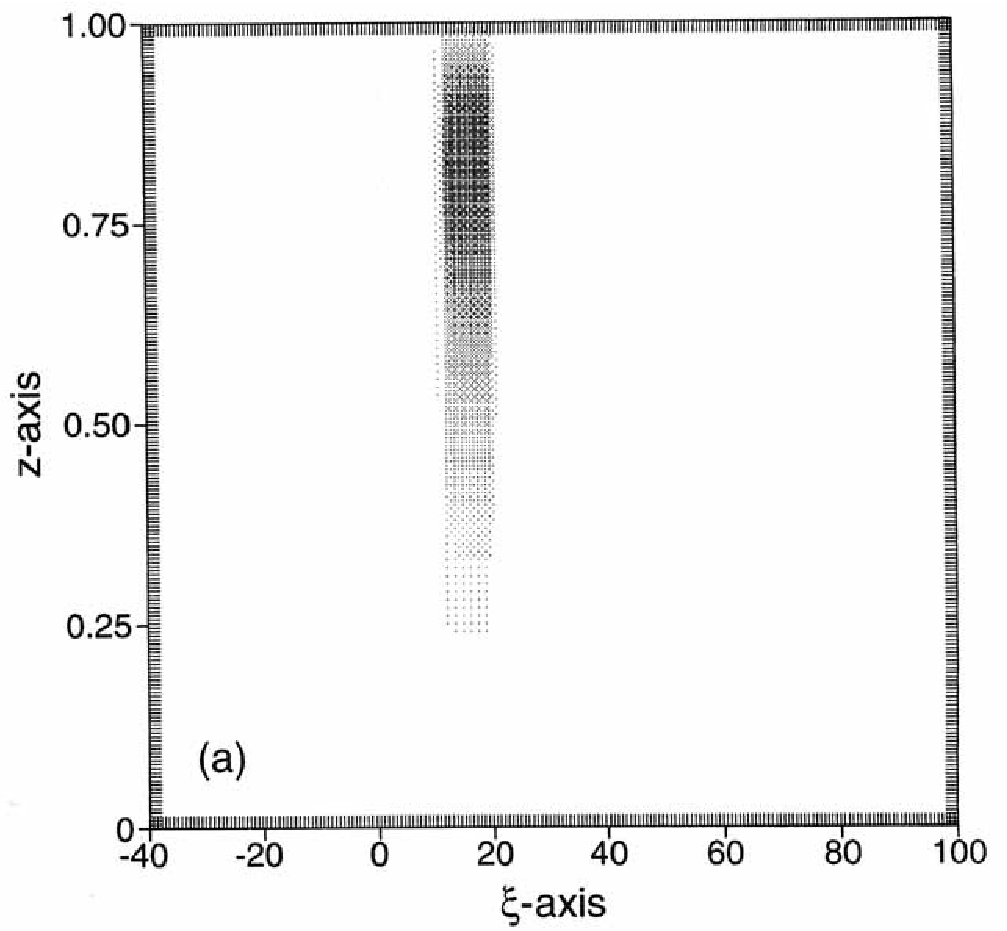

FIGURE 5 Gray-scale plots of the stream function for the same parameter values as in Figure 4. The gray intensity scales with the stream function amplitude.

regions near the left of each panel. The largest values in the stream function magnitude occur in the upper portion of the water column.

The final series of figures we present is for the vertical momentum flux. The dimensional vertical momentum flux, which we denote here as $\mathscr{F}^*$ in order to avoid confusion with the slow time variable τ, may be written in the form

$$\mathscr{F}^* \equiv \rho_* A_v \frac{\partial \omega^*_{\text{unif}}}{\partial z^*} = \mathscr{F}_* \mathscr{F}, \tag{4.4}$$

where

$$\mathscr{F}_* = \frac{\varepsilon 6 \rho_* A_v N^* H}{L\kappa}, \tag{4.5}$$

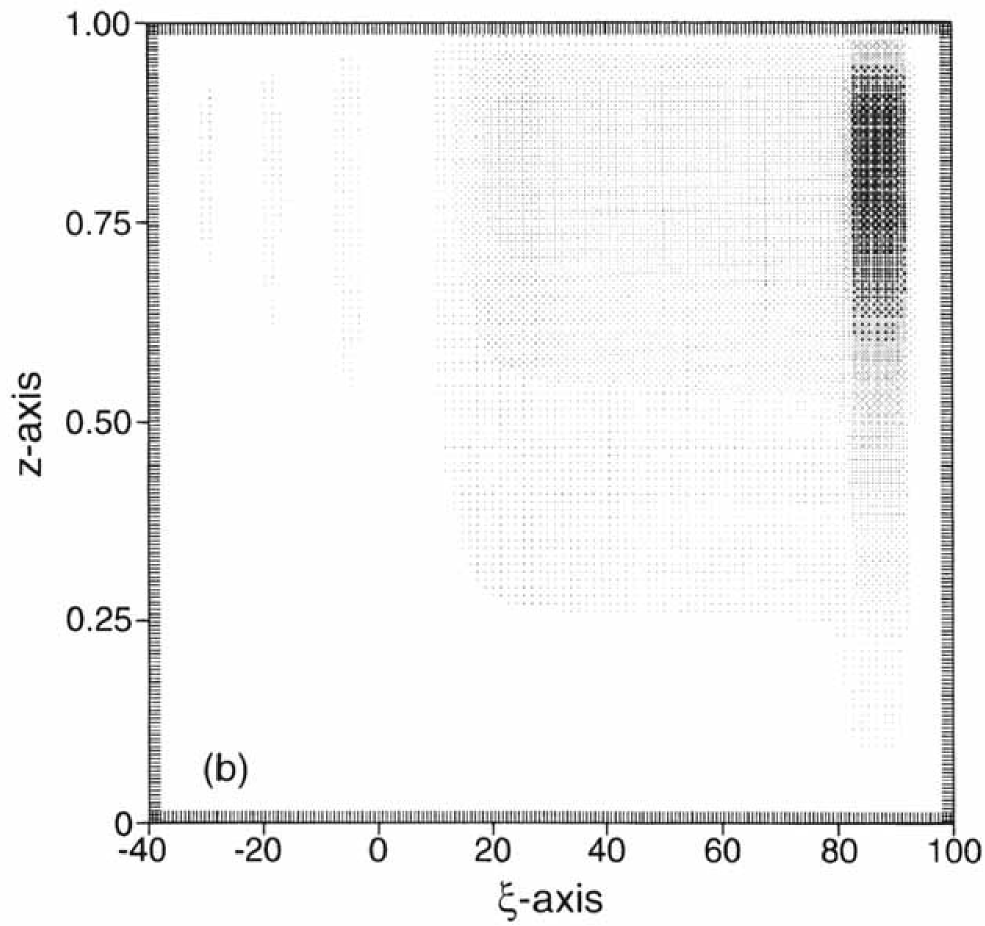

FIGURE 5 (Continued)

$$\mathscr{F}(z,\xi,T) = -\frac{\partial A_{\text{unif.}}(\xi,T)}{\partial\xi}\frac{\partial\phi_0(z)}{\partial z}. \tag{4.6}$$

For the scalings introduced in Section 2, it follows that $\mathscr{F}_* \simeq 1.85\times 10^{-4}\text{kgm}^{-1}\text{s}^{-2}$.

In Figure 6 we present gray-scale plots for $\mathscr{F}(z,\xi,T)$ for the same sequence of times and parameter values as in Figure 4. In order to highlight the contrast between the regions of upward and downward vertical momentum flux, we have chosen to shade only the regions of upward momentum flux and leave the regions of downward momentum flux unshaded. The horizontal nodal line located at approximately $z \simeq 0.6$ corresponds to the location of the maximum in the gravest vertical mode. The vertical nodal lines correspond to

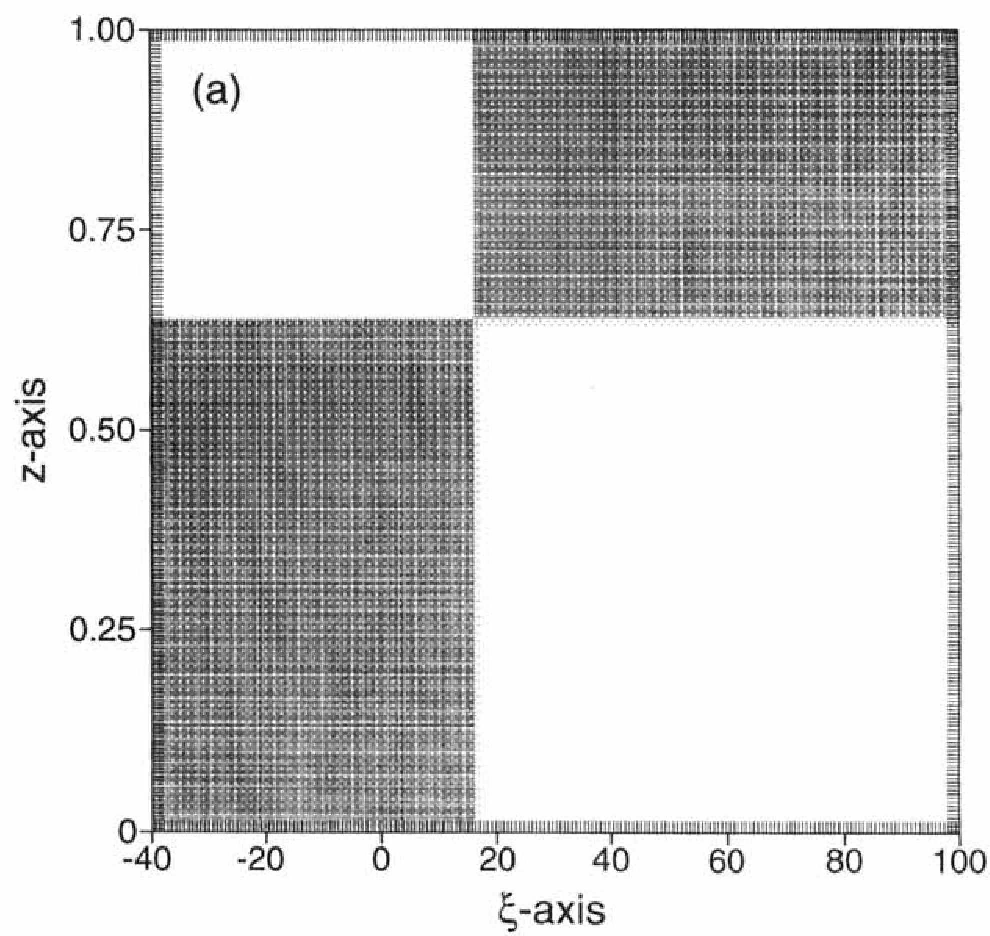

FIGURE 6 Gray-scale plots of the vertical momentum flux for the same parameter values as in Figure 4. The dark regions have upward momentum flux and the unshaded regions have downward momentum flux.

locations where $\partial A_{\text{unif}}(\xi, T)/\partial\xi = 0$. In particular, the most rightward vertical nodal line in the figures corresponds to the position of the maximum soliton amplitude. The banded structure seen in Figure 6b near the left of the panels depicts the relatively complex pattern in the vertical momentum flux associated with the dispersive wave tail.

5. CONCLUSIONS

Internal solitons provide one of the most important mechanisms by which nutrients are pumped from the lower water column into

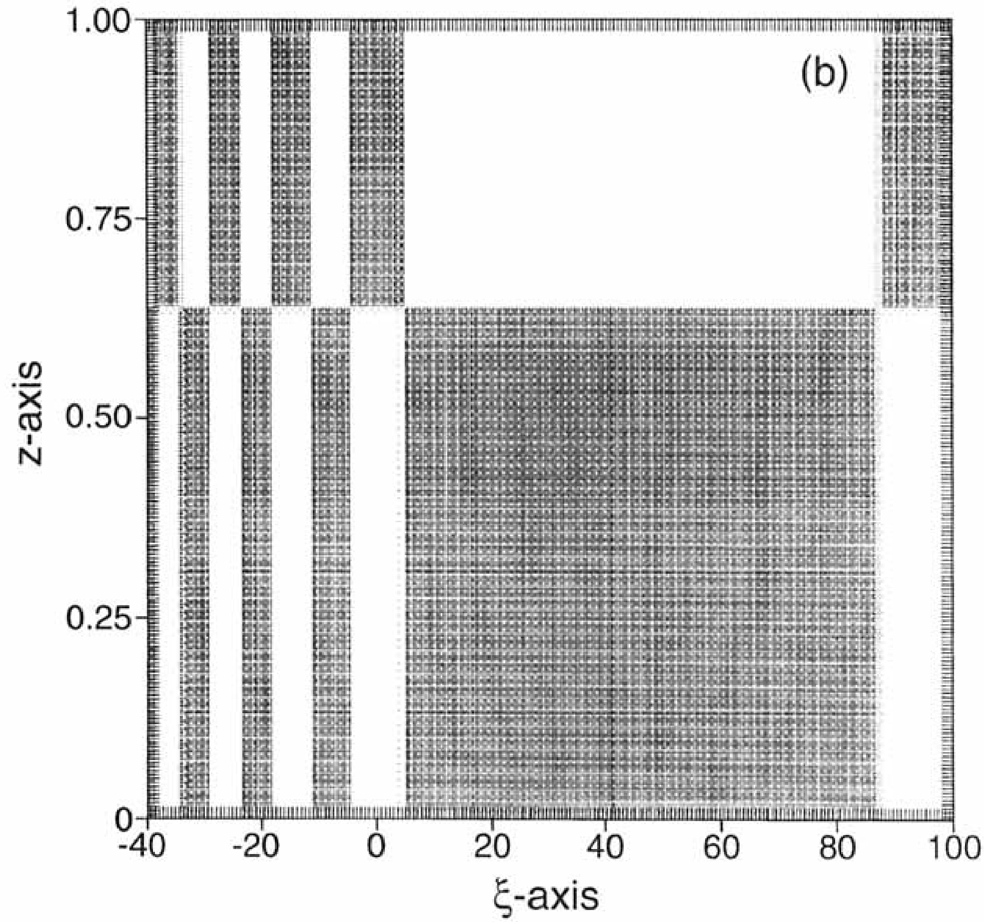

FIGURE 6 (Continued)

the upper water column in coastal seas. This effect can be enhanced by the dissipation of an internal soliton. Previous descriptions of the dissipation of an internal soliton have been based exclusively on an adiabatic assumption in which the soliton parameters continuously change in time according to an energy balance relation.

Our goal here has been to give a complete leading order description of a dissipating soliton including both horizontal and vertical dissipation. Our parameterization of the dissipation has been very crude in as much as we have adopted a simple eddy viscosity ansatz. Nevertheless, our analysis illustrated several key features of the structure of a dissipating internal soliton.

In particular, we have pointed out that the adiabatic ansatz breaks down when viewed in the context of an asymptotic expansion appropriate for weak dissipation. Physically, this breakdown is the consequence of the failure of the adiabatically decaying main pulse region to simultaneously satisfy averaged energy and mass balance relations. A so-called shelf region develops behind the travelling main pulse in order to compensate for the additional mass lost in the adiabatically decaying main pulse. We have explicitly constructed the leading order evolution of the shelf region and its connection to the first-order perturbation stream function field in the main pulse. The transition of the shelf region back to an undisturbed flow in the lee of the travelling internal soliton is accomplished through the formation of a spatially decaying packet of internal gravity waves corresponding to a similarity solution of the linearized KdV equation.

Acknowledgments

Preparation of this paper was supported in part by a Research Grant awarded by the Natural Sciences and Engineering Research Council of Canada and a Science Subvention awarded by the Department of Fisheries and Oceans of Canada to G.E.S. The award of a Teaching Assistantship by the Department of Mathematical Sciences to P.G.T. is gratefully acknowledged.

References

Benney, D. J., "Long nonlinear waves in fluid flows," *J. Math. Phys.* **45**, 52–63 (1966).

Bogucki, D. and Garrett, C., "A simple model for the shear-induced decay of an internal solitary wave," *J. Phys. Oceanogr.* **23**, 1767–1776 (1993).

Boyce, W. E. and DiPrima R. C., *Elementary Differential Equations and Boundary Value Problems*, 2nd ed., Wiley, 533 pp. (1969).

Briscoe, M. G., "Tides, solitons and nutrients," *Nature* **312**, 15 (1984).

Bryan, K. and Ripa, P., "The vertical structure of north Pacific temperature anomalies," *J. Geophys. Res.* **83**, 2419–2429 (1978).

Farmer, D. and Smith, J. D., "Nonlinear internal waves in a fjord," *Hydrodynamics of Estuaries and Fjords*, J. C. J. Nihoul, Ed., Elsevier, 465–493 (1978).

Fournier, R. O., Marra, J., Bohrer R. and van Det, M., "Plankton dynamics and nutrient enrichment of the Scotian shelf," *J. Fish. Res. Board Can.* **34**, 1004–1018 (1977).

Gear, J. A. and Grimshaw, R., "A second order theory for solitary waves in shallow fluids," *Phys. Fluids* **26**, 14–29 (1983).

Grimshaw, R. H. J., "Slowly-varying solitary waves. I. Korteweg-de Vries equation," *Proc. R. Soc. Lond.* **A 368**, 359–375 (1979).

Karpman, V. I. and Maslov, E. M., "Structure of tails produced under the action of perturbations on solitons," *Soviet Phys. JETP* **48**, 252–259 (1978).

Kaup, D. J. and Newell, A. C., "Solitons as particles and oscillators and in slowly-varying media: A singular perturbation theory," *Proc. R. Soc. Lond.* **A 361**, 413–446 (1978).

Knickerbocker, C. J. and Newell, A. C., "Internal solitary waves near a turning point," *Phys. Lett.* **75A**, 326–330 (1980a).

Knickerbocker, C. J. and Newell, A. C., "Shelves and the Korteweg-de Vries equation," *J. Fluid Mech.* **98**, 803–818 (1980b).

Kodama, Y. and Ablowitz, M. J., "Perturbations of solitons and solitary waves," *Stud. Appl. Math.* **64**, 225–245 (1980).

Koop, C. G. and Browand, F. K., "Instability and turbulence in a stratified fluid with shear," *J. Fluid Mech.* **93**, 135–159 (1979).

LeBlond, P. H., "On the damping of internal gravity waves in a continuously stratified ocean," *J. Fluid Mech.* **25**, 121–142 (1966).

LeBlond, P. H. and Mysak, L. A., *Waves in the Ocean,* Elsevier, 602 pp. (1978).

Leone, C., Segur, H. and Hammack, J. L., "Viscous decay of long internal solitary waves," *Phys. Fluids* **25**, 942–944 (1982).

Liu, A. K., "Analysis of nonlinear waves in the New York Bight," *J. Geophys. Res.* **93**, 12 317–12 329 (1988).

Liu, A. K. Holbrook, J. K. and Apel, J. R., "Nonlinear internal wave evolution in the Sulu Sea," *J. Phys. Oceanogr.* **15**, 1613–1624 (1985).

Liu, A. K., Pereira, N. R. and Ko, D. R. S., "Weakly interacting internal solitary waves in neighboring pycnoclines," *J. Fluid Mech.* **122**, 187–194 (1982).

Ott, E. and Sudan, R. N., "Damping of solitary waves," *Phys. Fluids* **13**, 1432–1434 (1970).

Sandstrom, H. and Elliott, J. A., "Internal tide and solitons on the Scotian Shelf: A nutrient pump at work," *J. Geophys. Res.* **89**, 6415–6426 (1984).

Sandstrom, H., Elliott, J. A. and Cochrane, N. A., "Observing groups of solitary internal waves and turbulence with BATFISH and echo sounder," *J. Phys. Oceanogr.* **19**, 987–997 (1989).

Swaters, G. E. and Mysak, L. A., "Topographically-induced baroclinic eddies near a coastline, with application to the northeast Pacific," *J. Phys. Oceanogr.* **15**, 1470–1485 (1985).

Swaters, G. E. and Sawatzky, R. P., "Viscoelastic modulation of solitary pressure pulses in nonlinear fluid-filled distensible tubes," *Q. J. Mech. Appl. Math.* **42**, 213–237 (1989).

Timko, P. G., "Turbulent dissipation of internal solitons," M.Sc. Thesis, Department of Mathematical Sciences, University of Alberta, 190 pp. (1995).